

Nonclassical properties of a deformed atom-cavity field state

Naveen Kumar, Deepak, Arpita Chatterjee*

*Department of Mathematics, J. C. Bose University of Science and Technology,
YMCA, Faridabad 121006, India*

Abstract

We analyze here a nonclassical state produced by an atom-cavity field interaction. The two-level atom is passed through the single-mode electromagnetic cavity field. By deforming the field operators and introducing nonlinearity to the classic Jaynes–Cummings model, we explore the system in respect of a nonlinear Hamiltonian. Assuming that the atom is in an excited state and the field is in a coherent state initially, the analytic expression for the state vector of the entire system state vector is obtained. With the help of the derived state vector, we calculate the photon number distribution, Mandel’s Q_M parameter, Wigner function, anti-bunching, squeezing properties and Q function etc.

1. Introduction

The conventional Jaynes–Cummings model (JCM) [1] describes the atom-cavity interaction as a two-level atom is colliding with a single mode of the electromagnetic field in the matter–radiation coupling. This model is proposed as a basic design to investigate the semiclassical behaviour of quantum radiation field [2]. The generalized Jaynes-Cummings model, illustrating the nonlinear interaction of a two or multi-level atom with a cavity field, results a deformed JCM structure. In quantum optics and quantum information processing [3], the nonclassical light field is of major interest for a number of reasons. In an all-optical quantum information processing device [4], the single-photon Fock state, a nonclassical state, is an essential resource. Controlling the emission of a single radiator, such as a molecule or a quanta [5], can be used to create these states. Fock state can also be prepared using

*Corresponding author

Email addresses: naveen74418@gmail.com (Naveen Kumar),
deepak20dalal19@gmail.com (Deepak), arpita.sps@gmail.com (Arpita Chatterjee)

cavity QED experiments in which atoms interact one at a time with a high Q resonator. A π quantum Rabi pulse in a microwave cavity [6] or an adiabatic passage sequence in an optical cavity [7] can produce a one-photon Fock state in this way. The study of these states yields a fundamental understanding of quantum fluctuations and a new method of quantum communication or imaging that surpasses the standard quantum noise limit. Nonclassical states have a wide range of real-world applications. For example, squeezed states are used to reduce the noise level in one of the phase-space quadratures below the quantum limit [8], entangled states are employed to realize a quantum computer and to transfer quantum information [9]. Here under the rotating-wave approximation (RWA), we investigate the dynamics of two-photon correlations generated by the interaction of a semiclassical two-level atom with a single-mode cavity field.

The following is a breakdown of the paper's structure. We begin by describing the interaction between a two-level atom and a single-mode field and solve the time-dependent Schrödinger equation [8], and derive the definite form of the atom-cavity state vector. To find the field's nonclassical properties, we first trace out the atom part from the atom-field system. We then check the nonclassicality criteria for distribution of photon numbers that means the probability of detecting n photons in the state $\hat{\rho}$. It is a smooth function of n for classical states like coherent and thermal states and an oscillating function of n for nonclassical states like squeezed states, as described in Schleich and Wheeler's [10] seminal work on interference in phase space. We further discuss the nonclassicality of the cavity field described by Mandel's Q_M parameter, Wigner function, anti-bunching, squeezing parameter, and Q function.

2. State of interest

In a typical Jaynes-Cummings model, a two-level atom interacts with a single-mode quantized electromagnetic field oscillating with frequency Ω . We consider $\sigma_{ij} = |i\rangle\langle j|$, ($i, j = 1, 2$) with $|2\rangle$ ($|1\rangle$) as the excited (ground) state of the atom. With these notations, the resonant Jaynes-Cummings Hamiltonian can be written as (with units such that $\hbar = 1$) [11, 12]

$$H = \Omega N + \omega \sigma_3 + g(a\sigma_{21} + a^\dagger \sigma_{12}) \quad (1)$$

where $N = a^\dagger a$ is the number operator for the electromagnetic field mode, $\sigma_3 = |2\rangle\langle 2| - |1\rangle\langle 1|$ is the atomic inversion operator, $\omega = \omega_2 - \omega_1$ is the atomic transition frequency, and the coupling constant g is effectively the product of the dipole moment and the mode function of the cavity mode

at the position of the atom. The first two terms of (1) are the free Hamiltonians of a single-mode electromagnetic field and a two-level atom. When the atom is interacting with the cavity field, it may drop (jump) from the excited (ground) to ground (excited) state by emitting (absorbing) a photon. The Hamiltonian (1) describes one of the few exactly solvable models in quantum optics. The deformation can be added to the atom-field system in two different ways. First, the field properties can be modified by an intensity-dependent coupling between the atom and the radiation field, i.e. the coupling is no longer linear in the field variables. Secondly, a system is considered in which the electromagnetic field mode is excited in a Kerr medium. This system may be realized by the experiment with a Rydberg atom in a nonlinear Kerr-like cavity. We consider here the first kind of nonlinearity only. The Hamiltonian describing the dynamics of this quantum system in the rotating wave approximation (RWA) is obtained from (1) by deforming the bosonic operators as

$$H = \Omega \hat{A}^\dagger \hat{A} + (\omega_1 \sigma_{11} + \omega_2 \sigma_{22}) + g(\hat{A} \sigma_{21} + \hat{A}^\dagger \sigma_{12}). \quad (2)$$

The f -deformed annihilation (\hat{A}) and creation (\hat{A}^\dagger) operators are constructed from the usual bosonic operators \hat{a} , \hat{a}^\dagger and the number operator $\hat{n} = \hat{a}^\dagger \hat{a}$ such as $\hat{A}^\dagger = f(\hat{n}) \hat{a}^\dagger$ and $\hat{A} = \hat{a} f(\hat{n})$, where $f(\hat{n})$ is an arbitrary real function of the number operator \hat{n} [13, 14]. One way of realizing nonlinear Jaynes-Cummings Hamiltonian is to consider atomic systems with vibrational sidebands [15]. The spatial structure of the cavity field determines the form for the function $f(\hat{a}^\dagger \hat{a})$. By proper choice of cavity mode structure, it is possible to design arbitrary atom-field couplings. Another way to arrive at atom-field coupling, which has polynomial dependence on the photon number, is to use many lasers with different phases and Rabi frequencies to interact with a trapped ion with vibrational sidebands [11]. The number of lasers required is same as the order of the polynomial. Once the specific form of the function $f(n)$, considered to be a polynomial, is fixed, the required phases and the Rabi frequencies of the external lasers can be determined. With the technological advancement in trapping and availability of lasers, it is possible to engineer the atom-environment coupling by varying laser frequencies and their intensities. Some f -deformed bosonic commutations relations are

$$\begin{aligned} [\hat{A}, \hat{A}^\dagger] &= (\hat{n} + 1) f^2(\hat{n} + 1) - \hat{n} f^2(\hat{n}) = g(\hat{n}), \text{ say} \\ [\hat{A}^\dagger \hat{A}, \hat{A}] &= -g(\hat{n}) \hat{A}, \quad [\hat{A}^\dagger \hat{A}, \hat{A}^\dagger] = \hat{A}^\dagger g(\hat{n}) \\ [\hat{A}^\dagger \hat{A}, \hat{A}^\dagger g(\hat{n})] &= \hat{A}^\dagger g^2(\hat{n}), \quad [\hat{A}^\dagger \hat{A}, \hat{A}^\dagger g^p(\hat{n})] = \hat{A}^\dagger g^{p+1}(\hat{n}) \\ [\hat{A}^\dagger \hat{A}, -g(\hat{n}) \hat{A}] &= g^2(\hat{n}) \hat{A}, \quad [\hat{A}^\dagger \hat{A}, (-1)^p g^p(\hat{n}) \hat{A}] = (-1)^{p+1} g^{p+1}(\hat{n}) \hat{A} \end{aligned}$$

The Hamiltonian in the interaction picture is

$$H_r = e^{iH_{r0}t} H_{r1} e^{-iH_{r0}t}$$

where

$$\begin{aligned} H_{r0} &= \Omega \hat{A}^\dagger \hat{A} + w_1 \sigma_{11} + w_2 \sigma_{22} \\ H_{r1} &= g(\hat{A} \sigma_{21} + \hat{A}^\dagger \sigma_{12}) \end{aligned}$$

Applying the Baker-Campbell-Hausdorff formula, H_r can be calculated as

$$\begin{aligned} H_r &= H_{r1} + (it)[H_{r0}, H_{r1}] + \frac{(it)^2}{2!}[H_{r0}, [H_{r0}, H_{r1}]] + \frac{(it)^3}{3!}[H_{r0}, [H_{r0}, [H_{r0}, H_{r1}]]] + \dots \\ &= \sum_{r=0}^{\infty} \frac{(it)^r}{r!} [H_0, [H_0, [H_0, \dots H_1]]]_r \text{ times} \end{aligned} \quad (3)$$

and thus the effective Hamiltonian as

$$H_{\text{eff}} = g[e^{-ith(\hat{n})} A \sigma_{21} + A^\dagger e^{ith(\hat{n})} \sigma_{12}] \quad (4)$$

where $h(\hat{n}) = \Omega f^2(\hat{n}) + (\omega_2 - \omega_1)$.

Solving the Schrödinger equation of motion [8]

$$i \frac{\partial |\psi\rangle}{\partial t} = H |\psi\rangle, \quad (5)$$

for any arbitrary state $|\psi\rangle = \sum C_{1,n+1}(t)|1, n+1\rangle + C_{2,n}(t)|2, n\rangle$, $|2\rangle$ and $|1\rangle$ are the excited and ground states of atom, respectively, the equations of motion in terms of the probability amplitudes of the state vector $|\psi\rangle$ are

$$\dot{C}_{2,n+1}(t) = e^{ih(\hat{n})t} \sqrt{n+1} C_{1,n}(t),$$

$$\dot{C}_{1,n}(t) = e^{-ih(\hat{n})t} \sqrt{n+1} C_{2,n+1}(t).$$

Assuming that the atom enters the cavity in its excited state $|2\rangle$ and the radiation field is initially in a coherent state, that means $C_{1,n}(0) = 0$ and $C_{2,n+1}(0) = C_n(0) = e^{-\frac{|\beta|^2}{2}} \frac{\beta^n}{\sqrt{n!}}$, the above equations can be solved as

$$C_{2,n+1}(t) = \frac{e^{-\frac{|\beta|^2}{2}} \beta^n}{\sqrt{n!}(m_2 - m_1)} \{m_2 e^{m_1 t} - m_1 e^{m_2 t}\} \quad (6)$$

$$C_{1s,n}(t) = \frac{e^{-ih(n)t} m_1 m_2 e^{-\frac{|\beta|^2}{2}} \beta^n}{\sqrt{n!} \sqrt{n+1} g f(n+1) (m_2 - m_1)} \{e^{m_1 t} - e^{m_2 t}\} \quad (7)$$

where

$$2m_{1,2} = ih(n) \pm i\sqrt{4g^2(n+1)f^2(n+1) + h^2(n)}$$

The state vector $|\psi(t)\rangle$ for an arbitrary state describes the time evolution of the whole atom-field system. Here we focus on some analytical properties of the single-mode cavity field, which is obtained from $|\psi(t)\rangle$ by tracing out the atom part

$$\rho(t)_f = \text{Tr}_a[\rho(t)], \quad (8)$$

where the subscript a (f) denotes the atom (field). We consider $\rho(t)_f$ throughout the paper for determining the properties of the field left into the cavity. The general form of the expectation $\langle a^{\dagger p} a^q \rangle$ with respect to the state vector $|\psi\rangle$ can be calculated as follows:

$$\begin{aligned} \langle a^{\dagger p} a^q \rangle &= \langle \psi | a^{\dagger p} a^q | \psi \rangle \\ &= \sum_n \left[C_{2,n+p-q+1}^*(t) C_{2,n+1}(t) \frac{\sqrt{(n+p-q+1)!(n+1)!}}{(n+1-q)!} \right. \\ &\quad \left. + C_{1,n+p-q}^*(t) C_{1,n}(t) \frac{\sqrt{(n+p-q)!n!}}{(n-q)!} \right] \end{aligned} \quad (9)$$

3. Nonclassicality criteria under study

In this section, we derive some criteria to witness the nonclassicality of the considered quantum state $|\psi\rangle$. While plotting different distribution functions, the numerical values of the atomic transition frequencies and the coupling constant are chosen in such a way that they are in a weak coupling regime ($g \ll \omega_i$, $i = 1, 2$), which is the primary assumption for applying RWA. For simplicity, three different forms of $f(\hat{n})$, being an arbitrary polynomial function of \hat{n} , are considered. The following plots correspond to the cases $f(n) = \sin(n)$, $1/\sin(n)$, and $\ln(n)$. Here, $\sin(n)$ is a bounded and periodic polynomial function, $1/\sin(n)$ is an unbounded, periodic polynomial function and $\ln(n)$ is an unbounded, non-periodic, monotonically increasing polynomial function. In the limiting case $f(\hat{n}) = 1$, the Hamiltonian reduces to the basic Jaynes-Cummings model.

3.1. Photon number distribution

Photon number distribution is the probability distribution for finding n photons in a given cavity field. It can be found as the expectation of the density field with respect to the number state n as

$$p(n) = \langle n | \hat{\rho} | n \rangle \quad (10)$$

After tracing out the atom part, the density operator $\hat{\rho}_f$ is given by

$$\begin{aligned}\hat{\rho}_f &= |\psi\rangle_f \langle\psi| \\ &= \sum_n \left[|C_{2,n+1}(t)|^2 |n+1\rangle\langle n+1| + C_{2,n+1}(t)C_{1,n}^*(t) |n+1\rangle\langle n| \right. \\ &\quad \left. + C_{2,n+1}^*(t)C_{1,n}(t) |n\rangle\langle n+1| + |C_{1,n}(t)|^2 |n\rangle\langle n| \right]\end{aligned}\quad (11)$$

Substituting (11) into (10), the photon number distribution for the cavity field is obtained as

$$\begin{aligned}p(n) &= \langle n|\hat{\rho}|n\rangle \\ &= |C_{2,n+1}(t)|^2 + |C_{1,n}(t)|^2\end{aligned}\quad (12)$$

Here (12) gives the probability of finding n photons in a given cavity field state. The simplified form of photon number distribution can be plotted in Fig. 1 for three different functional values of $f(n)$, namely $\sin(n)$, $1/\sin(n)$ and $\ln(n)$. We can conclude from Fig. 1 that the variations of $p(n)$ with

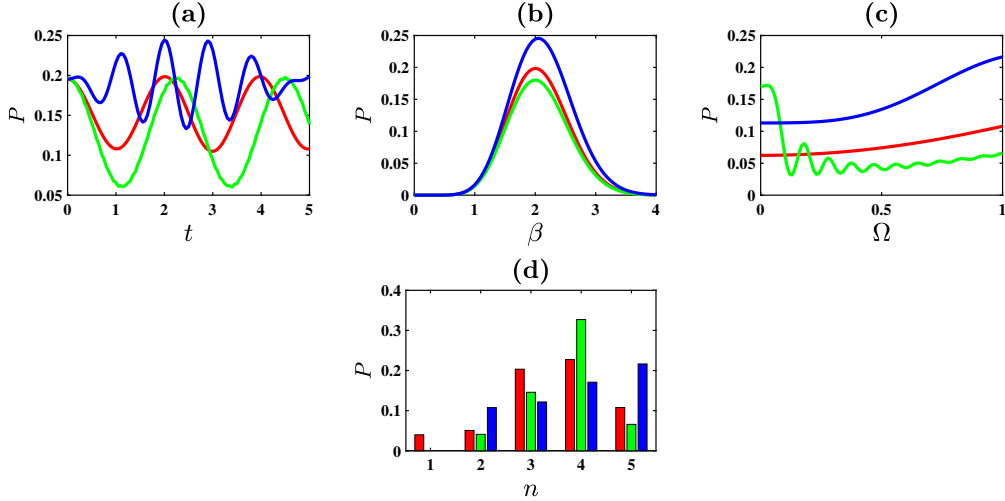


Figure 1: Variation of $p(n)$ with respect to (a) t and for $g = 0.5$, $\beta = 2$, $\Omega = 1\text{GHz}$, $\omega_1 = \omega_2 = 100\text{J}$, $n = 5$, (b) β and for $t = 1\text{hr}$, $g = 0.5$, $\Omega = 1\text{GHz}$, $\omega_1 = \omega_2 = 100\text{J}$, $n = 5$, (c) Ω and for $t = 1\text{hr}$, $g = 0.5$, $\beta = 2$, $\omega_1 = \omega_2 = 100\text{J}$, $n = 5$, (d) n and for $t = 1\text{hr}$, $g = 0.5$, $\beta = 2$, $\Omega = 1\text{GHz}$, $\omega_1 = \omega_2 = 100\text{J}$. Red, green, and blue lines represent $f(n) = \sin(n)$, $1/\sin(n)$, and $\ln(n)$ respectively.

respect to t , Ω follow wave nature and the amplitude of waves is maximum for $\ln(n)$ and minimum for $1/\sin(n)$. The variation of $p(n)$ with respect to β is first increasing and then decreasing and maximum value attained is 0.25. It can be further observed that the peak of $p(n)$ is highest (lowest) for

$f(n) = \ln(n)$ ($1/\sin(n)$). While plotting $p(n)$ for different number of photons n , all the three functions almost coincide for $n = 1$ and have distinct nature for $n > 1$.

3.2. Mandel's Q_M parameter

Sub-Poissonian photon statistics are one of the most striking nonclassical characteristics of a quantum system. Mandel's Q_M parameter, which measures how far the photon number distribution deviates from the Poissonian statistics, is used to determine such characteristics [16]. Q_M is zero for a coherent field, and the minimal value $Q_M = -1$ is obtained for Fock states, having a well-defined number of photons by definition. The field statistics is sub-Poissonian if $-1 \leq Q_M < 0$, and thus the phase space distribution cannot be interpreted as a classical probability function. As a result, the negative values of Q_M is sufficient for a field to be nonclassical. But the negativity of Q_M is not a necessary condition to distinguish the quantum states into nonclassical and classical regimes. For example, a state may be nonclassical even though Q_M is positive. If $Q_M > 0$, the state's statistics is super-Poissonian but no conclusions can be drawn about their character, for example the Q_M parameter for a well-known nonclassical thermal field is always positive. Next to determine the photon statistics of a single-mode radiation field, we consider the Mandel's Q_M parameter defined by

$$Q_M = \frac{\langle a^{\dagger 2} a^2 \rangle}{\langle a^{\dagger} a \rangle} - \langle a^{\dagger} a \rangle \quad (13)$$

Mandel's Q_M function can be plotted for different $f(n)$ such as $\sin n$, $1/\sin(n)$, and $\ln(n)$ with respect to different parameters in Fig. 2.

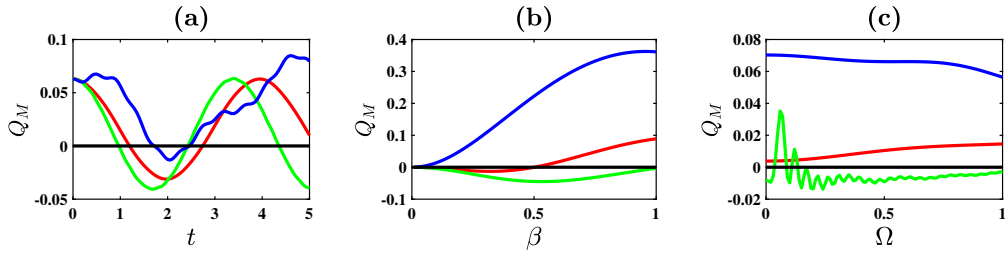


Figure 2: Variation of Q_M with respect to (a) t and for $g = 0.5$, $\beta = 2$, $\Omega = 1\text{GHz}$, $\omega_1 = \omega_2 = 100\text{J}$, (b) β and for $t = 1\text{hr}$, $g = 0.5$, $\Omega = 1\text{GHz}$, $\omega_1 = \omega_2 = 100\text{J}$, (c) Ω and for $t = 1\text{hr}$, $g = 0.5$, $\beta = 2$, $\omega_1 = \omega_2 = 100\text{J}$. Red, green, and blue lines represent $f(n) = \sin(n)$, $1/\sin(n)$, and $\ln(n)$ respectively.

Here we can observe that Q_M follows wavy nature with respect to t with maximum amplitude when $f(n) = \ln(n)$. Further Q_M shows nonclassicality

for all these three functions with respect to all the parameters along with $\ln(n)$ has minimum nonclassicality whereas $1/\sin(n)$ has maximum nonclassicality. Thus, in general we can conclude that the considered quantum state is nonclassical in nature for different polynomial functional values of $f(n)$ and order of nonclassicality may increase or decrease according to the choice of $f(n)$. Also the nonclassicality decreases with increasing of β , Ω and wavy in nature while increasing t .

3.3. Wigner function

The nonclassicality of a quantum state can be studied in terms of its phase-space distribution characterized by the Wigner function. For a quantum state $\hat{\rho}$, the Wigner function of the system is defined in terms of the coherent state basis as [8, 17, 18]

$$W(\gamma, \gamma^*) = \frac{2}{\pi^2} e^{2|\gamma|^2} \int d^2\delta \langle -\delta | \hat{\rho} | \delta \rangle e^{-2(\beta^* \delta - \beta \delta^*)},$$

where $|\delta\rangle = \exp(-|\delta|^2/2 + \delta \hat{a}^\dagger) |0\rangle$ is a coherent state. By using the relation [19]

$$\sum_{n=k}^{\infty} n_{C_k} y^{n-k} = (1-y)^{-k-1},$$

the Wigner function can be expressed in series form as [20]

$$W(\gamma, \gamma^*) = \frac{2}{\pi} \sum_{k=0}^{\infty} (-1)^k \langle \gamma, k | \hat{\rho} | \gamma, k \rangle, \quad (14)$$

where $|\gamma, k\rangle$ is the usual displaced number state. The partial negative value of the Wigner function is a one-sided condition for the nonclassicality of the related state [21], in the sense that one cannot conclude the state is classical when the Wigner function is positive everywhere. For example, the Wigner function of the squeezed state is Gaussian and positive everywhere but it is a well-known nonclassical state. For a classical state, a necessary but not sufficient condition is the positivity of the Wigner function. Hence, a state with a negative region in the phase-space quadrature is essentially nonclassical. Now the displaced number state $|\gamma, k\rangle$ can be expressed in a number state basis as

$$\begin{aligned} |\gamma, k\rangle &= D(\gamma) |k\rangle \\ &= e^{-\frac{|\gamma|^2}{2}} \sum_{m=0}^k \frac{\gamma^{*m}}{m!} \sqrt{\frac{k!}{(k-m)!}} \sum_{p=0}^{\infty} \frac{\gamma^p}{p!} \sqrt{\frac{(k-m+p)!}{(k-m)!}} |k-m+p\rangle \end{aligned} \quad (15)$$

Thus

$$\begin{aligned}
& \langle \gamma, k | n \rangle \\
&= e^{-\frac{|\gamma|^2}{2}} \sum_{m=0}^k \frac{(-\gamma)^m}{m!} \sqrt{\frac{k!}{(k-m)!}} \sum_{p=0}^{\infty} \frac{\gamma^{*p}}{p!} \sqrt{\frac{(k-m+p)!}{(k-m)!}} \langle k-m+p | n \rangle \\
&= e^{-\frac{|\gamma|^2}{2}} \sqrt{\frac{k!}{n!}} (\gamma^*)^{n-k} L_k^{(n-k)}(|\gamma|^2)
\end{aligned} \tag{16}$$

where $L_m^{(k)}(x) = \sum_{n=0}^m \frac{(-x)^n (m+k)!}{(m-n)! n! (k+n)!}$ is the associated Laguerre polynomial [22]. Substituting (16) into (14) we get

$$\begin{aligned}
W(\gamma, \gamma^*) &= \frac{2e^{-|\gamma|^2}}{\pi} \sum_{k=0}^{\infty} (-1)^k k! \sum_{n=0}^{\infty} \left[|c_{a,n}|^2 \frac{|\gamma|^{2(n-k)}}{n!} \left\{ L_k^{(n-k)}(|\gamma|^2) \right\}^2 \right. \\
&\quad \left. + |c_{b,n+1}|^2 \frac{|\gamma|^{2(n+1-k)}}{(n+1)!} \left\{ L_k^{(n+1-k)}(|\gamma|^2) \right\}^2 \right]
\end{aligned} \tag{17}$$

Here it is clear that the Wigner function shows the non-gaussian [23] be-

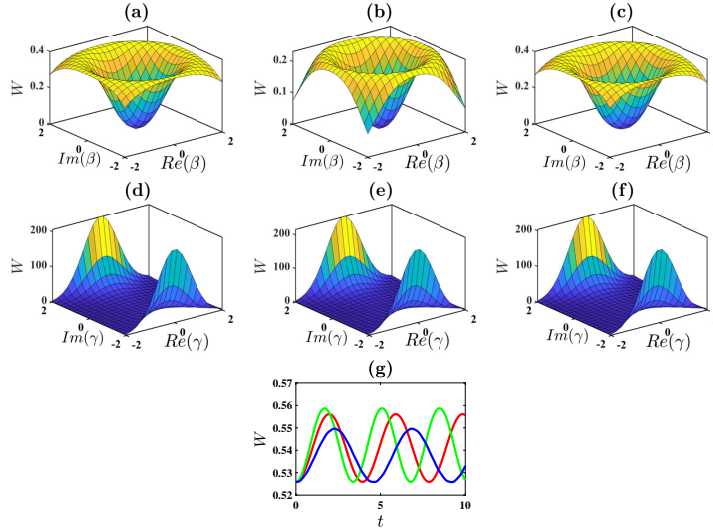


Figure 3: Variation of W with respect to β (γ) in the first (second) row and for $f(n) = \sin(n)$ in (a) and (d), $1/\sin n$ in (b) and (e), $\ln n$ in (c) and (f). W is plotted with respect to t in (g). Other parameters are the same as in Fig. 1.

haviour with respect to real and imaginary β and γ . As the Wigner function has no negative region, we can conclude that this function is not showing nonclassicality. Also the variation of Wigner function with respect to the parameter t shows wavy nature.

3.4. Anti-bunching

The theory of majorization in [24, 25] gives us the expression of anti-bunching in a quantum state which satisfies the condition for nonclassicality as

$$d_{(1)} = \langle a^{\dagger 2} a^2 \rangle - \langle a^{\dagger} a \rangle^2 < 0$$

The negativity of $d_{(1)}$ implies that the probability of detecting independent photons is more than the clustered photons. We can find the expression of $d_{(1)}$ by using the expectation values of $a^{\dagger 2} a^2$ and $a^{\dagger} a$ from (9). Also the anti-bunching criteria can be plotted in Fig. 4 with respect to different parameters. It is seen that anti-bunching has the similar behaviour as Q_M .

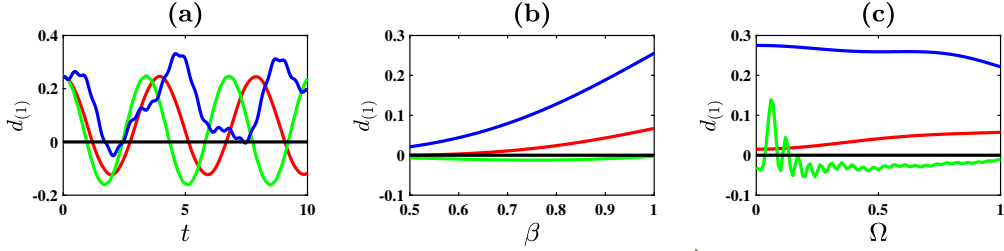


Figure 4: Variation of $d_{(1)}$ for different $f(n)$ and with respect to (a) t , (b) β and (c) Ω . Other parameters are the same as in Fig. 1.

3.5. Squeezing properties

In order to analyze the quantum fluctuations of the field quadratures, we consider two Hermitian operators which are combinations of photon creation and annihilation operators as

$$x = \frac{a + a^{\dagger}}{2}, \quad p = \frac{a - a^{\dagger}}{2i}$$

with the commutation relation $[x, p] = i/2$. They obey the Heisenberg uncertainty relation of the form $\langle (\Delta x)^2 \rangle \langle (\Delta p)^2 \rangle \geq \frac{1}{16}$, and thus the quadrature squeezing occurs whenever $\langle (\Delta x)^2 \rangle < \frac{1}{4}$ or $\langle (\Delta p)^2 \rangle < \frac{1}{4}$. It is convenient to introduce the squeezing parameters as [26]

$$\begin{aligned} s_x &= 4\langle (\Delta x)^2 \rangle - 1 \\ &= 2\langle a^{\dagger} a \rangle + \langle a^2 \rangle + \langle a^{\dagger 2} \rangle - \langle a \rangle^2 - \langle a^{\dagger} \rangle^2 - 2\langle a \rangle \langle a^{\dagger} \rangle, \end{aligned}$$

and

$$s_p = 4\langle (\Delta p)^2 \rangle - 1$$

$$= 2\langle a^\dagger a \rangle - \langle a^2 \rangle - \langle a^{\dagger 2} \rangle + \langle a \rangle^2 + \langle a^\dagger \rangle^2 - 2\langle a \rangle \langle a^\dagger \rangle,$$

such that the squeezing exists in x or p quadrature if $-1 < s_x < 0$ or $-1 < s_p < 0$, respectively. The negativity of squeezing is not a necessary condition but a sufficient one. The expectations can be calculated using (9). In Fig. 5 we observe that the squeezing parameters $S = s_x, s_p$ are positive

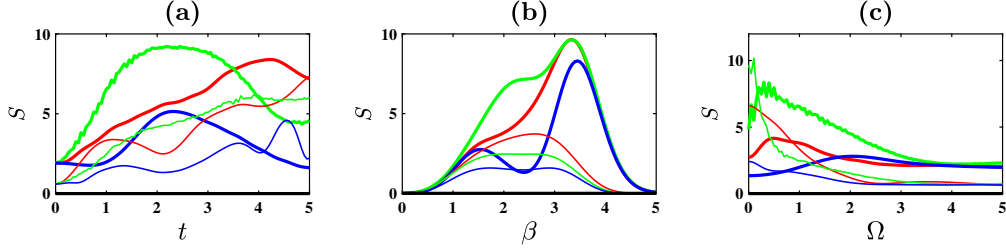


Figure 5: Variation of Squeezing parameters $S = s_x$ (thick line) and s_p (thin line) with respect to t in (a), β in (b) and Ω in (c). Other parameters are the same as in Fig. 1.

for all parametric values of t , β , and Ω and thus they fail to detect the nonclassical nature of the cavity field.

3.6. Q Function

The uncertainty principle prevents a direct phase-space description of a quantum mechanical system. This fact leads to the creation of quasiprobability distributions, which are very useful in quantum mechanics because they provide a quantum-classical correspondence and make it easier to calculate quantum mechanical averages in a way that is similar to the calculation of classical phase-space averages [27]. The Q function is one such quasiprobability distribution, and its zeros are a sign of nonclassicality [28]. The Q function is calculated as follows:

$$\begin{aligned} Q &= \frac{1}{\pi} \langle \alpha | \rho | \alpha \rangle \\ &= \langle \alpha | \sum_{n,p} [C_{1,n+1} C_{1,p+1}^* |n+1\rangle \langle p+1| + C_{2,n} C_{2,p}^* |n\rangle \langle p|] | \alpha \rangle \\ &= \sum_{n,p} [C_{1,n+1} C_{1,p+1}^* e^{-\frac{|\alpha|^2}{2}} \frac{\alpha^{*(n+1)}}{\sqrt{(n+1)!}} e^{-\frac{|\alpha|^2}{2}} \frac{\alpha^{p+1}}{\sqrt{(p+1)!}} + C_{2,n} C_{2,p}^* e^{-\frac{|\alpha|^2}{2}} \frac{\alpha^{*(n)}}{\sqrt{(n)!}} e^{-\frac{|\alpha|^2}{2}} \frac{\alpha^p}{\sqrt{p!}}] \\ &= e^{-|\alpha|^2} \sum_{n,p} \left[\frac{\alpha^{*n} \alpha^p}{\sqrt{p!n!}} \left\{ C_{1,n+1} C_{1,p+1}^* \frac{|\alpha|^2}{\sqrt{(p+1)(n+1)}} + C_{2,n} C_{2,p}^* \right\} \right] \end{aligned}$$

In Fig. 6, we observe that the Q distribution shows the wavy and non-Gaussian nature and remains positive everywhere.

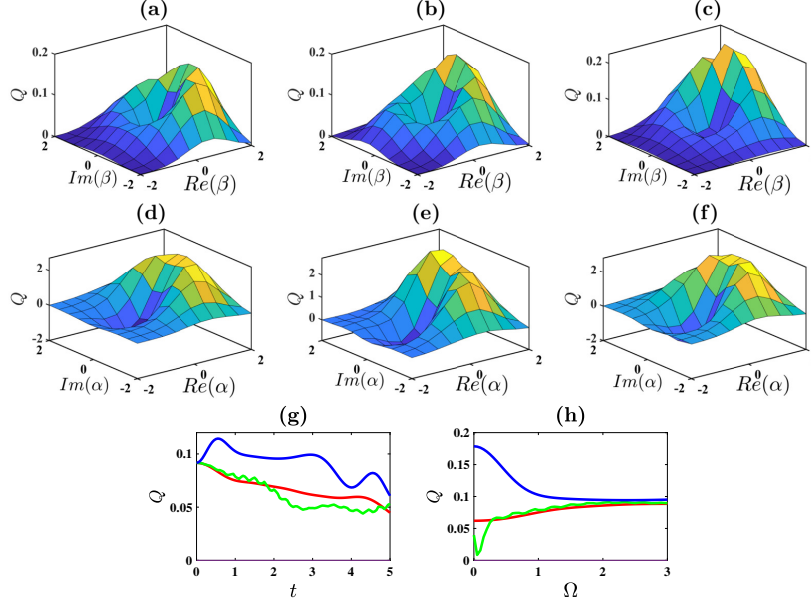


Figure 6: Variation of Q with respect to β (α) in the first (second) row and for $f(n) = \sin(n)$ in (a) and (d), $1/\sin n$ in (b) and (e), $\ln n$ in (c) and (f). Q is plotted with respect to t in (g) and Ω in (h). Other parameters are the same as in Fig. 1.

4. Conclusion

In this article, we have considered a deformed model of interaction between a two-level atom and a single-mode electromagnetic cavity field. Assuming that the atom enters the cavity in its excited state $|2\rangle$ and the field is initially in a coherent state, we have derived the cavity field state. For this cavity field state, we have found some statistical properties like photon number distribution, Wigner function, Mandel's Q_M parameter, anti-bunching, squeezing parameter, and Q -function. All of these criteria have specific conditions for witnessing nonclassicality such as the negativity of the lower-order antibunching and the Poissonian statistics of Mandel's Q_M parameter are used to reveal the nonclassicality of the quantum field state. Here we have observed that the Q -function, Wigner function, and squeezing parameter failed to show nonclassicality.

ACKNOWLEDGEMENT

Naveen and Deepak acknowledge the financial support from the Council of Scientific and Industrial Research, Govt. of India (Grant no. 09/1256(0004)/2019-EMR-I and 09/1256(0006)/2019-EMR-I, respectively).

References

- [1] E. T. Jaynes, F. W. Cummings, Proc. IEEE. 51, 89 (1963).
- [2] B. W. Shore, P. L. Knight, J. Mod. Opt. 40, 1195 (1993).
- [3] D. Bouwmeester, A. Ekert, A. Zeilinger, *The Physics of Quantum Information*, Berlin: Springer (2000).
- [4] E. Knill, R. Laflamme, G. J. Milburn, Nature, 409, 46 (2001).
- [5] C. Brunel, B. Lounis, P. Tamarat, M. Orrit, Phys. Rev. Lett. 83, 2722 (1999).
- [6] X. Maître, E. Hagley, G. Nogues, C. Wunderlich, P. Goy, M. Brune, J.M. Raimond, S. Haroche, Phys. Rev. Lett. 79, 769 (1997).
- [7] M. Hennrich, T. Legero, A. Kuhn, G. Rempe, Phys. Rev. Lett. 85, 4872 (2000).
- [8] M. O. Scully, M. S. Zubairy, *Quantum Optics*, Cambridge University Press (1997).
- [9] S. L. Braunstein, P. van Loock, Rev. Mod. Phys. 77, 513–577 (2005).
- [10] W. Schleich, J. A. Wheeler, Nature 326, 574 (1987).
- [11] S. Sivakumar, Int. J. Theor. Phys. 43, 2405-2421 (2004).
- [12] C. Cohen-Tannoudji, J. Dupont-Roc, G. Grynberg, *Atom-Photon Interactions; Basic Processes and Applications*, John Wiley and Sons, New York (1992).
- [13] V. I. Mańko, G. Marmo, E. C. G. Sudarshan, F. Zaccaria, Phys. Scr. 55, 528 (1997).
- [14] R. A. Zait, Phys. Lett. 319, 461 (2003).
- [15] R. L. de Matos Filo, W. Vogel, Phys. Rev. A 58, 2326 (1998).
- [16] L. Mandel, Opt. Lett. 4, 205 (1979).
- [17] P. K. Pathak, G. S. Agarwal, Phys. Rev. A 71, 043823 (2005).
- [18] A. Chatterjee, J. Mod. Opt. 59 (9), 814 (2012).

- [19] M. Abramowitz, I. A. Stegun, *Handbook of Mathematical Functions*, New York: Dover (1972).
- [20] H. Moya-Cessa P. L. Knight, Phys. Rev. A 48, 2479 (1993).
- [21] Z. Wang, H. C. Yuan, H. Y. Fan, J. Opt. Soc. Am. B 28, 1964 (2011).
- [22] G. S. Agarwal, K. Tara, Phys. Rev. A 43(1), 492 (1991).
- [23] P. Malpani, K.thapliyal, J. Banerji, A. Pathak, [arXiv:2109.12145v1](#) (2021).
- [24] C. T. Lee, Phys. Rev. A 41, 1721 (1990).
- [25] A. Pathak, M. E. Garcia, Appl. Phys. B 84, 479 (2006).
- [26] A. Chatterjee, R. Ghosh, J. Opt. Soc. Am. B 33(7), 1511 (2016).
- [27] K. Thapliyal, S. Banerjee, A. Pathak, S. Omkar, V. Ravishankar, Ann. Phys. 362, 261 (2015).
- [28] N. Lütkenhaus, S. M. Barnett, Phys. Rev. A 51, 3340 (1995).